PERTURBATIONS OF A SPACECRAFT ORBIT DURING AN HYPERBOLIC FLYBY

Nicole J. Rappaport, Giacomo Giampieri, and John D. Anderson

Submitted to Icarus - 27 Mars 2000
28 pages, 3 figures, 0 table

ABSTRACT

A first-order perturbation theory exists for the flyby problem with the Born approximation as the reference orbit (Anderson and Giampieri 1999). This theory is applicable when the flyby can be approximated by a straight line, a hyperbola with zero bending angle or infinite eccentricity, but it fails when the central mass GM is large, or when the flyby is at a small distance b or a small velocity v. The applicability of the theory depends on the parameter GM/bv^2 being small. Here we present an analytical theory for the motion of a spacecraft with the hyperbola as the reference orbit. The perturbations consist of the next term after the monopole in the central body's exterior gravitational potential function, the quadrupole terms, which we represent by the usual harmonic coefficients C_{20} and C_{22}. These harmonic coefficients are the only coefficients of degree two that need be considered when the gravity harmonic coefficients are referred to the principal axis system of the body. The perturbations of the hyperbolic elements are expressed as functions of the unperturbed values of the elements. There are no approximations with respect to the eccentricity or inclination, hence the equations for the variation of the elements do not involve infinite series. We compare results of the new theory with results of numerical integration and with results predicted by the Anderson-Giampieri theory (AGT). We find that we can improve the orbital accuracy of AGT by a simple modification, and we correct a sign error in the C_{22} term in the AGT potential function.

PERTURBATIONS OF A SPACECRAFT ORBIT DURING AN HYPERBOLIC FLYBY

Nicole J. Rappaport, Giacomo Giampieri, and John D. Anderson

Submitted to Icarus - 27 Mars 2000
Revised - 16 October 2000

35 pages, 4 figures, 0 table

Dr. Nicole J. Rappaport
Jet Propulsion Laboratory
Mail Stop 301-150
California Institute of Technology
Pasadena CA 91109 USA
E-mail: Nicole.J.Rappaport@jpl.nasa.gov
Tel: (818) 354 8211
Fax: (818) 393 6388

Dr. Giacomo Giampieri
Imperial College of Science, Technology and Medecine
Space and Atmospheric Physics Group
The Blackett Laboratory
Imperial College
London SW7 2BW United Kingdom
E-mail: g.giampieri@ic.ac.uk
Tel: 44 (0) 20 7594 7775
Fax: 44 (0) 20 7594 7772

Dr. John D. Anderson
Jet Propulsion Laboratory
Mail Stop 238-420
California Institute of Technology
Pasadena CA 91109 USA
E-mail: John.D.Anderson@jpl.nasa.gov
Tel: (818) 354 3956
Fax: (818) 354 6825

Proposed Running Title:
ORBITAL PERTURBATIONS DURING AN HYPERBOLIC FLYBY

KEY WORDS: Celestial Mechanics, Orbits, Planetary Dynamics

ABSTRACT

A first-order perturbation theory exists for the flyby problem with the Born approximation as the reference orbit (Anderson and Giampieri 1999, AG thereafter). This theory is applicable when the deflection parameter μ/bv^2 (where μ is the product of the gravitational constant by the body's mass, b the impact parameter, and v the velocity of the flyby) is small. Here we present an analytical theory for the motion of a spacecraft with the hyperbola as the reference orbit. The perturbations consist of the next term after the monopole in the central body's gravitational exterior potential function, represented by the quadrupole harmonic coefficients C_{20} and C_{22}. The perturbations of the hyperbolic elements are expressed in closed form, without involving infinite series, as functions of the unperturbed orbital elements. We compare results of the new theory with the AG's theory. We find that the AG's theory can be improved by a simple modification, and by correcting a sign error in the C_{22} term in the potential function. The effects of the body's rotation on the perturbations are discussed, and new results pertaining to the AG's approach are given.

1. INTRODUCTION

This paper deals with the perturbations of the trajectory of a spacecraft during a close flyby of a non spherical central mass distribution, in particular a satellite or a planet.

The motivation and justification for the paper are presented in section 2. The equations of Lagrange for the hyperbolic motion are derived in section 3. The first order solution with respect to the body's gravity harmonic coefficients of degree two, C_{20} and C_{22}, is presented in section 4. Section 5 compares the new theory with the Anderson Giampieri or AG theory (1999) as well as with results of numerical integrations. Both the new theory and the AG's theory neglect the effect of the body's rotation on the perturbations due to its quadrupole moments. Section 6 discusses this assumption and presents a modification of the AG's theory that yields the effects of the rotation. Section 7 contains our conclusion.

Appendix A summarizes pertinent equations for the unperturbed hyperbolic motion.

2. MOTIVATION AND JUSTIFICATION

The work presented in this paper was motivated by the need to study spacecraft flybys of planetary bodies from the point of view of using such flybys to measure the body's gravitational field, and to improve our knowledge of the ephemerides of planetary bodies and spacecraft.

Over the past few years, analyses of spacecraft Doppler data have allowed scientists to determine the gravity field of the Jupiter's Galilean satellites (Anderson et al. 1996a, 1996b, 1997a, 1997b) and infer important (and surprising) new information on their interiors. Gravity science of Saturn and its satellites is an important goal of the Cassini mission. So, we started this work with an interest in the flybys that will occur with the Cassini Orbiter spacecraft during its tour of the Saturnian system.

Although the JPL Orbit Determination Program (ODP) can be used for simulations and covariance analyses, an analytical theory is useful in a complementary way

to provide more insight for focused studies, and to compare efficiently a large number of tour and observation possibilities in support of Cassini mission and experiment planning.

Within the last decade, an elegant general satellite perturbation theory has appeared that can easily be extended to hyperbolic orbits (Gooding 1992). However, because we are dealing here with a limited number of gravitational harmonics for icy satellites, or for the giant outer planets, the implementation of Gooding's theory, with all its generalities, is not necessarily the most efficient way to proceed. Instead, we have chosen to implement a simpler first-order perturbation theory, useful for mission simulations of Doppler tracking experiments in the outer solar system.

More recently, a very simple analytical theory has been developed for flybys of small bodies (Anderson and Giampieri 1999 or AG), which also uses the method of variation of parameters, but which adopts unperturbed orbital elements based on the Born approximation for a massless central body. In the AG's theory, all gravity terms are treated as perturbations, including the monopole coefficient μ, the product of the gravitational constant and the total mass of the central body. The unperturbed motion is rectilinear and uniform.

The AG's theory is based on the assumption that the parameter $\varepsilon = \mu/bv^2 << 1$, where b is the impact parameter, and v is the speed of the spacecraft with respect to the body at closest approach. This assumption is verified in the example of section 5, in which we have $\varepsilon \approx 7.1 \times 10^{-2}$, but is only marginally verified in the example of the Pioneer 11 flyby of Saturn, for which $\varepsilon \approx 0.46$. By contrast, the new theory, which does not assume such a small parameter, has a general domain of applicability.

Practical examples show that the AG's theory does not compute mass perturbations with sufficient accuracy for targeted flybys of satellites of the giant planets of the solar system. However, we found that we could improve the calculation of the mass perturbations in the AG's theory. This is presented in section 5.1.

Furthermore, the comparisons between the new and AG theories allowed us to identify and correct a sign error in section 6.2 of the AG's paper, "Quadrupole Sectorial Harmonics." This error and subsequent errors that result from it are corrected in section 5.2 of this paper.

The corrected and improved AG's theory is now such that, for small ε, the flyby trajectories that it predicts agree remarkably well with those computed from both numerical integrations and the hyperbolic theory of this paper.

For purposes of performing mission studies, we have implemented both theories, as well as a strictly numerical theory based on numerical integration of the equations of motion. With these three tools, we are able to provide reliable flyby simulations of gravity-science experiments for practically any mission scenario. Although the actual experiment must be performed with the ODP, or its equivalent, mission studies can be done with greater efficiency and flexibility by implementing the results of this paper.

3. VARIATIONS OF PARAMETERS

In this section, we derive the Lagrange equations for the hyperbolic motion, following and adapting the derivation of Battin (1987) of the Lagrange equation for the elliptical motion.

We use the classical hyperbolic orbital elements defined by Battin (1987) page 165. Let us consider the reference frame $Ox'y'z'$ such that:

1. O coincides with the focus of the hyperbola;
2. Oz' is normal to the orbit;
3. Ox' is in the direction of the vertix (periapsis).

The semi-major axis ($a < 0$) and eccentricity ($e > 1$) define the shape of the orbit in this reference frame in terms of the cylindrical coordinates r (radius) and f (true anomaly) by

$$r = \frac{a(1-e^2)}{1+e\cos f}. \tag{1}$$

The longitude of the node Ω, inclination I, and argument of pericenter ω are the Euler angles orienting the reference frame $Ox'y'z'$ with respect to the body-fixed reference frame $Oxyz$.

The mean motion n and mean anomaly M are defined in a similar way as for the elliptic motion by

$$n = \sqrt{\frac{\mu}{(-a)^3}}, \tag{2}$$

and

$$M = n(t - t_{c/a}) = nt + \Lambda, \tag{3}$$

where $t_{c/a}$ is the time of passage at periapsis.

Useful properties of the hyperbolic orbits are given in Appendix A.2.1.

3.1. Fundamental Equations

The method of the variation of parameters writes the equations of motion in the form

$$L\frac{d\vec{\alpha}}{dt} = \left(\frac{\partial \mathcal{R}}{\partial \vec{\alpha}}\right)^T, \tag{4}$$

where the Lagrange matrix L is defined by

$$L_{ij} = [\alpha_i, \alpha_j]; \tag{5}$$

where $\mathcal{R}$ is the disturbing function, and the $[\alpha_i, \alpha_j]$ are Lagrange brackets, defined by:

$$[\alpha_i, \alpha_j] = \frac{\partial \vec{r}}{\partial \alpha_i} \cdot \frac{\partial \vec{v}}{\partial \alpha_j} - \frac{\partial \vec{r}}{\partial \alpha_j} \cdot \frac{\partial \vec{v}}{\partial \alpha_i}. \tag{6}$$

3.2. Lagrange Brackets

Using fundamental equations given in Appendix A, we compute the Lagrange brackets. The ones which are different from zero are

$$
\begin{aligned}
[a,\Omega] &= -\frac{1}{2}na\sqrt{e^2-1}\cos I, \\
[a,\omega] &= -\frac{1}{2}na\sqrt{e^2-1}, \\
[a,\Lambda] &= \frac{1}{2}na, \\
[e,\Omega] &= -\frac{na^2 e\cos I}{\sqrt{e^2-1}}, \\
[e,\omega] &= -\frac{na^2 e}{\sqrt{e^2-1}}, \\
[I,\Omega] &= na^2\sqrt{e^2-1}\sin I,
\end{aligned}
\tag{7}
$$

The Lagrange brackets given by Eq. (7) are similar to those for the elliptic motions but have $\sqrt{1-e^2}$ replaced by $\sqrt{e^2-1}$ and different signs, depending on the Lagrange bracket.

3.3. Equations of Motion

Using Eqs. (7) and inverting Eqs. (4), we obtained the Lagrange equations for the hyperbolic motion in the form

$$
\begin{aligned}
\frac{da}{dt} &= -\frac{2}{na}\frac{\partial \mathcal{R}}{\partial \Lambda}, \\
\frac{de}{dt} &= \frac{\sqrt{e^2-1}}{na^2 e}\frac{\partial \mathcal{R}}{\partial \omega} + \frac{(e^2-1)}{na^2 e}\frac{\partial \mathcal{R}}{\partial \Lambda}, \\
\frac{dI}{dt} &= -\frac{1}{na^2\sqrt{e^2-1}\sin I}\frac{\partial \mathcal{R}}{\partial \Omega} + \frac{\cos I}{na^2\sqrt{e^2-1}\sin I}\frac{\partial \mathcal{R}}{\partial \omega}, \\
\frac{d\Omega}{dt} &= \frac{1}{na^2\sqrt{e^2-1}\sin I}\frac{\partial \mathcal{R}}{\partial I}, \\
\frac{d\omega}{dt} &= -\frac{\sqrt{e^2-1}}{na^2 e}\frac{\partial \mathcal{R}}{\partial e} - \frac{\cos I}{na^2\sqrt{e^2-1}\sin I}\frac{\partial \mathcal{R}}{\partial I}, \\
\frac{d\Lambda}{dt} &= \frac{2}{na}\frac{\partial \mathcal{R}}{\partial a} - \frac{(e^2-1)}{na^2 e}\frac{\partial \mathcal{R}}{\partial e}
\end{aligned}
\tag{8}
$$

The terms in the right-hand side members of the Lagrange equations given by Eq. (8) are similar to those for the elliptic motions but have $\sqrt{1-e^2}$ replaced by $\sqrt{e^2-1}$ and different signs, depending on the term.

To deal with the case of zero inclination, we introduce the classical non-singular variables

$$
\begin{aligned}
P &= \tan\frac{I}{2}\sin\Omega, \\
Q &= -\tan\frac{I}{2}\cos\Omega.
\end{aligned}
\tag{9}
$$

whose variations are governed by the equations

$$
\begin{aligned}
\frac{dP}{dt} =& \frac{1}{2}\left(1+\tan^2\frac{I}{2}\right)\sin\Omega\frac{dI}{dt} + \tan\frac{I}{2}\cos\Omega\frac{d\Omega}{dt} \\
=& \frac{1}{na^2\sqrt{e^2-1}\sin I}\left\{\frac{1}{2}\left(1+\tan^2\frac{I}{2}\right)\sin\Omega\left[-\frac{\partial\mathcal{R}}{\partial\Omega}+\cos I\frac{\partial\mathcal{R}}{\partial\omega}\right]+\right. \\
& \left.\tan\frac{I}{2}\cos\Omega\frac{\partial\mathcal{R}}{\partial I}\right\}, \\
\frac{dQ}{dt} =& -\frac{1}{2}\left(1+\tan^2\frac{I}{2}\right)\cos\Omega\frac{dI}{dt} + \tan\frac{I}{2}\sin\Omega\frac{d\Omega}{dt} \\
=& \frac{1}{na^2\sqrt{e^2-1}\sin I}\left\{-\frac{1}{2}\left(1+\tan^2\frac{I}{2}\right)\cos\Omega\left[-\frac{\partial\mathcal{R}}{\partial\Omega}+\cos I\frac{\partial\mathcal{R}}{\partial\omega}\right]+\right. \\
& \left.\tan\frac{I}{2}\sin\Omega\frac{\partial\mathcal{R}}{\partial I}\right\}.
\end{aligned}
\tag{10}
$$

We do not consider in this paper the case of eccentricities equal to 1 as this case is not relevant in practice for the flybys we are considering.

4. VARIATION OF THE ELEMENTS FOR THE PERTURBATIONS DUE TO C_{20} AND C_{22}

In this section, we compute the variations of the hyperbolic elements due to C_{20} and C_{22}. This is useful to evaluate the perturbations of the quadrupole gravitational field of the body in the case where the gravity harmonic coefficients are referred to the principal axis system of the body. This assumption is most useful for a body (e.g., a satellite) which orbits in a synchronous fashion on a low inclination-, low eccentricity-orbit around a primary (e.g., a planet). In that case, we can assume that the axis of lower inertia is along the direction from the body's center to the primary's center.

4.1. Disturbing Function

4.1.1. General Formulation

The disturbing function can be written as:

$$\mathcal{R} = \frac{\mu}{r} \sum_{\ell=1}^{+\infty} \sum_{m=1}^{\ell} \left(\frac{R}{r}\right)^{\ell} P_{lm}(\sin\varphi) \left(C_{\ell m} \cos m\lambda + S_{\ell m} \sin m\lambda\right), \tag{11}$$

at radius r, latitude φ, and longitude λ; R is the reference radius and the $P_{\ell m}$ are Legendre functions.

Eq. (11) can be expressed in terms of orbital elements using the relation

$$\begin{aligned} P_{\ell m}(\sin\varphi)\exp(m\lambda) = & \begin{pmatrix} 1 \\ -i \end{pmatrix} \begin{matrix} (\ell-m) \text{ even} \\ (\ell-m) \text{ odd} \end{matrix} \sum_{p=0}^{\ell} F_{\ell m p}(I) \\ & \exp i\left[(\ell-2p)(\omega+f) + m(\Omega-\theta)\right], \end{aligned} \tag{12}$$

where the Kaula functions of the inclination (Kaula, 1966) are defined by:

$$\begin{aligned} F_{\ell m p}(I) = & \frac{(-1)^{\left[\frac{\ell-m}{2}\right]}(\ell+m)!}{2^{\ell}\ell!} \binom{\ell}{p} \sum_{j=\max(0,2p-\ell-m)}^{\min(\ell-m,2p)} (-1)^{j} \binom{2p}{j} \binom{2\ell-2p}{\ell-m-j} \\ & \left(\cos\frac{I}{2}\right)^{\ell-m-j} \left(\sin\frac{I}{2}\right)^{l-m+2p-2j}. \end{aligned} \tag{13}$$

and θ is the angle orienting the x-axis with respect to an inertial axis in the equatorial plane of the body.

4.1.2. Degree 2 Disturbing Function

We select the satellite body-fixed reference frame to coincide with the principal axes of inertia of the body. In that reference frame, all the gravity coefficients of degree two, except C_{20} and C_{22}, vanish. The disturbing function of degree two is composed of two terms

$$\mathcal{R}_{20} = \frac{\mu}{r}\left(\frac{R}{r}\right)^2 C_{20}\left\{[F_{201}(I) + 2F_{200}(I)\cos(A_{200} + 2f)]\right\}, \tag{14}$$

and

$$\begin{aligned}\mathcal{R}_{22} =& \frac{\mu}{r}\left(\frac{R}{r}\right)^2 C_{22}\Big\{F_{220}(I)\cos(A_{220} + 2f) + F_{222}(I)\cos(A_{222} + 2f) + \\ & F_{221}(I)\cos(A_{221})\Big\},\end{aligned} \tag{15}$$

where the angles are defined by

$$A_{\ell mp} = (\ell - 2p)\omega + m(\Omega - \theta), \tag{16}$$

and with the functions of the inclination I

$$\begin{aligned} F_{201}(I) &= \frac{3}{4}\sin^2 I - \frac{1}{2}, \\ F_{200}(I) = F_{202}(I) &= -\frac{3}{8}\sin^2 I, \\ F_{220}(I) &= \frac{3}{4}(1 + \cos I)^2, \\ F_{222}(I) &= \frac{3}{4}(1 - \cos I)^2, \\ F_{221}(I) &= \frac{3}{2}\sin^2 I, \end{aligned} \tag{17}$$

4.2. Variations of the Elements

We computed the first order variations of the hyperbolic elements of the spacecraft's trajectory by replacing in the right-hand side member of the equations of motion the

hyperbolic elements by their unperturbed values and integrating the equations obtained in this way.

The only assumption that we made was that $\theta \equiv \theta_0$ is constant during a flyby. In other words we neglected the rotation of the body during the duration of the flyby. This assumption, which was made for simplicity, is justified in the cases where the duration of the flyby is smaller than the rotation rate of the body. We discuss this assumption in more details in section 6.

Furthermore, the direct effects of the centrifugal and Coriolis forces associated with the rotation of the body are not the subject of this paper. For covariance analyses, these forces are not important since they have no effect on the observable. For trajectory calculations, the rotation perturbations derived by Anderson and Giampieri (1999) can be used to introduce the rotation perturbations into the body-fixed principal axes.

The derivation started from indefinite integrals over time, transformed to true anomaly. The analytical integration of the last equation turned out to be very complicated, due in particular to the presence of terms in $H\cos(jf)$ and $H\sin(jf)$ where H is the hyperbolic eccentric anomaly (see Appendix A.2.1).

Below are our results, giving the variations of the elements with respect to the body-fixed reference frame at closest approach. We use the subscript "i" to denote initial values, and the subscript "0" to denote unperturbed values. We designate by $A^0_{\ell mp}$ the value of $A_{\ell mp}$ computed with ω_0, Ω_0, and θ_0.

There is no approximation with respect to the eccentricity or the inclination. The equations given below for the variations of the hyperbolic elements do not involve any infinite series.

The semi-major axis is given by:

$$\begin{aligned} a =& a_1 + \left(\frac{R^2}{a_0}\right)\left\{C_{20}\left[F_{201}(I_0)G_{a1}(e_0,f_0) + 2F_{200}(I_0)G_{a2}(e_0,A^0_{200},f_0)\right] + \right. \\ & C_{22}\left[F_{220}(I_0)G_{a2}(e_0,A^0_{220},f_0) + F_{222}(I_0)G_{a2}(e_0,-A^0_{222},f_0) + \right. \\ & \left.\left. F_{221}(I_0)G_{a1}(e_0,f_0)\cos(A^0_{221})\right]\right\}, \end{aligned} \tag{18}$$

where a_1 is a constant of integration and with

$$G_{a1}(e,f) = -\frac{1}{2(e^2-1)^3}\Big[(12e+3e^3)\cos f + 6e^2\cos 2f + e^3\cos 3f\Big],$$

$$\begin{aligned} G_{a2}(e,x,f) = -\frac{1}{4(e^2-1)^3}\Big[&e^3\cos(x-f) + (12e+3e^3)\cos(x+f) + \\ &(8+12e^2)\cos(x+2f) + (12e+3e^3)\cos(x+3f) + 6e^2\cos(x+4f) + \\ &e^3\cos(x+5f)\Big]. \end{aligned} \tag{19}$$

The eccentricity is given by

$$\begin{aligned} e =& e_1 + \left(\frac{R}{a}\right)^2\Big\{C_{20}\Big[F_{201}(I_0)G_{e1}(e_0,f_0) + 2F_{200}(I_0)G_{e2}(e_0,A^0_{200},f_0)\Big] + \\ &C_{22}\Big[F_{220}(I_0)G_{e2}(e_0,A^0_{220},f_0) + F_{222}(I_0)G_{e2}(e_0,-A^0_{222},f_0) + \\ &F_{221}(I_0)G_{e1}(e_0,f_0)\cos(A^0_{221})\Big]\Big\}, \end{aligned} \tag{20}$$

where e_1 is a constant of integration and with

$$G_{e1}(e,f) = -\frac{(e^2-1)}{2e}G_{a1}(e,f)$$

$$\begin{aligned} G_{e2}(e,x,f) = -\frac{(e^2-1)}{2e}G_{a2}(e,x,f) + \frac{1}{3e(e^2-1)}\Big[&3e\cos(x+f) + 3\cos(x+2f) + \\ &e\cos(x+3f)\Big]. \end{aligned} \tag{21}$$

The argument of periapsis is given by:

$$\omega = \omega_1 + \left(\frac{R}{a_0}\right)^2 \left\{ C_{20} \left[F_{201}(I_0) G_{\omega 1}(e_0, f_0) + 2F_{200}(I_0) G_{\omega 2}(e_0, A^0_{200}, f_0) + \right.\right.$$
$$\left. \cot I_0 \left(\frac{dF_{201}}{dI_0}(I_0) \tilde{G}_{\omega 1}(e_0, f_0) + 2\frac{dF_{200}}{dI_0}(I_0) \tilde{G}_{\omega 2}(e_0, A^0_{200}, f_0) \right) \right] +$$
$$C_{22} \left[F_{220}(I_0) G_{\omega 2}(e_0, A^0_{220}, f_0) + F_{222}(I_0) G_{\omega 2}(e_0, -A^0_{222}, f_0) + \right. \tag{22}$$
$$F_{221} G_{\omega 1}(e_0, f_0) \cos(A^0_{221}) + \cot I_0 \left(\frac{dF_{220}}{dI_0}(I_0) \tilde{G}_{\omega 2}(e_0, A^0_{220}, f_0) + \right.$$
$$\left.\left. \left. \frac{dF_{222}}{dI_0}(I_0) \tilde{G}_{\omega 2}(e_0, -A^0_{222}, f_0) + \frac{dF_{221}}{dI_0}(I_0) \tilde{G}\omega 1(e_0, f_0) \cos(A^0_{221}) \right) \right] \right\},$$

where ω_1 is a constant of integration and with

$$G_{\omega 1}(e, f) = \frac{1}{4e(e^2-1)^2} \left[12ef + (12 + 9e^2) \sin f + 6e \sin 2f + e^2 \sin 3f \right]$$

$$G_{\omega 2}(e, x, f) = \frac{1}{24e(e^2-1)^2} \left[-3e^2 \sin(x - f) + (-12 + 21e^2) \sin(x + f) + \right.$$
$$36e \sin(x + 2f) + (28 + 11e^2) \sin(x + 3f) + 18e \sin(x + 4f) +$$
$$\left. 3e^2 \sin(x + 5f) \right], \tag{23}$$

$$\tilde{G}_{\omega 1}(e, f) = -\frac{1}{e(e^2-1)^2} \left[ef + e^2 \sin f \right],$$

$$\tilde{G}_{\omega 2}(e, x, f) = -\frac{1}{6e(e^2-1)^2} \left[3e^2 \sin(x + f) + 3e \sin(x + 2f) + e^2 \sin(x + 3f) \right].$$

The inclination and longitude of the node can be computed from the equations

$$
\begin{aligned}
P =& P_1 + \left(\frac{R}{a}\right)^2 \left\{ C_{20} \left[\tilde{F}_0(I_0) \left(G_{P1}(e_0, A^0_{201} + \Omega_0, f_0) + G_{P2}(e_0, A_{200} + \Omega_0, f_0) \right) \right] + \right. \\
& C_{22} \left[\tilde{F}_1(I_0) \left(G_{P1}(e_0, -A^0_{221} + \Omega_0, f_0) + G_{P2}(e, A^0_{220} + \Omega_0, f_0) \right) + \right. \\
& \left. \left. \tilde{F}_2(I_0) \left(G_{P1}(e_0, A^0_{221} + \Omega_0, f_0) + G_{P2}(e, -A^0_{222} + \Omega_0, f_0) \right) \right] \right\},
\end{aligned}
\tag{24}
$$

$$
\begin{aligned}
Q =& Q_1 + \left(\frac{R}{a}\right)^2 \left\{ C_{20} \left[\tilde{F}_0(I_0) \left(G_{Q1}(e_0, A^0_{201} + \Omega_0, f_0) + G_{Q2}(e_0, A_{200} + \Omega_0, f_0) \right) \right] + \right. \\
& C_{22} \left[\tilde{F}_1(I_0) \left(G_{Q1}(e_0, -A^0_{221} + \Omega_0, f_0) + G_{Q2}(e, A^0_{220} + \Omega_0, f_0) \right) + \right. \\
& \left. \left. \tilde{F}_2(I_0) \left(G_{Q1}(e_0, A^0_{221} + \Omega_0, f_0) + G_{Q2}(e, -A^0_{222} + \Omega_0, f_0) \right) \right] \right\},
\end{aligned}
\tag{25}
$$

where P_1 and Q_1 are constants of integration and with

$$
\begin{aligned}
\tilde{F}_0(I) =& \frac{3}{2} \tan\left(\frac{I}{2}\right) \cos I, \\
\tilde{F}_1(I) =& \frac{3}{2} \tan\left(\frac{I}{2}\right) (1 + \cos I), \\
\tilde{F}_2(I) =& \frac{3}{2} \tan\left(\frac{I}{2}\right) (-1 + \cos I),
\end{aligned}
\tag{26}
$$

and

$$G_{P1}(e,x,f) = \frac{\cos(x)}{(e^2-1)^2}\left[f + e\sin f\right],$$

$$G_{P2}(e,x,f) = -\frac{1}{6(e^2-1)^2}\left[3e\sin(x+f) + 3\sin(x+2f) + e\sin(x+3f)\right],$$

$$G_{Q1}(e,x,f) = \frac{\sin(x)}{(e^2-1)^2}\left[f + e\sin f\right], \tag{27}$$

$$G_{Q2}(e,x,f) = \frac{1}{6(e^2-1)^2}\left[3e\cos(x+f) + 3\cos(x+2f) + e\cos(x+3f)\right].$$

The variable Λ is given by:

$$\begin{aligned}\Lambda =& \Lambda_1 + \left(\frac{R}{a}\right)^2 \Bigg\{ C_{20}\Big[F_{201}(I_0)G_{\Lambda 1}(e_0, f_0, H_0, M_i) + \\ & 2F_{200}(I_0)G_{\Lambda 2}(e_0, A^0_{200}, f_0, H_0, M_i)\Big] + \\ & C_{22}\Big[F_{220}(I_0)G_{\Lambda 2}(e_0, A^0_{220}, f_0, H_0, M_i) + F_{222}(I_0)G_{\Lambda 2}(e_0, -A^0_{222}, f_0, H_0, M_i) + \\ & F_{221}(I_0)G_{\Lambda 1}(e_0, f_0, H_0, M_i)\cos(A^0_{221})\Big]\Bigg\},\end{aligned} \tag{28}$$

$$G_{\Lambda 1}(e,f,H,M) =$$
$$\frac{1}{4e(e^2-1)^{5/2}}\Big[-(12-3e^2+6e^4)\sin f-(6e+6e^3)\sin 2f-(e^2+2e^4)\sin 3f\Big]+$$
$$\frac{3(M+H)}{4(e^2-1)^3}\Big[(12e+3e^3)\cos f+6e^2\cos 2f+e^3\cos 3f\Big]+$$
$$\frac{3}{2(e^2-1)^3}\Big[-(6e+3e^2+2e^3)M+(2+3e^2)H\Big],$$

$$G_{\Lambda 2}(e,x,f,H,M) =$$
$$\frac{1}{24e(e^2-1)^{5/2}}\Big[(3e^2+6e^4)\sin(x-f)+(16+18e-32e^2+18e^3+16e^4)\sin(x)+$$
$$(12+39e^2-6e^4)\sin(x+f)-(28+7e^2+10e^4)\sin(x+3f)-$$
$$(18e+18e^3)\sin(x+4f)-(3e^2+6e^4)\sin((x+5f)\Big]+$$
$$\frac{3(M+H)}{8(e^2-1)^3}\Big[e^3\cos(x-f)+(12e+3e^3)\cos(x+f)+(8+12e^2)\cos(x+2f)+$$
$$(12e+3e^3)\cos(x+3f)+6e^2\cos(x+4f)+e^3\cos(x+5f)\Big]+$$
$$\frac{3}{4(e^2-1)^3}\Big[-(4+12e+9e^2+4e^3)M+3e^2H\Big]\cos(x). \tag{29}$$

The mean anomaly is given by

$$M(t) = M_i + n[a_p(t)](t-t_i) + \Lambda. \tag{30}$$

Next, we describe how the theory presented in this section should be applied to compute the hyperbolic orbital elements of the spacecraft at any time during the flyby.

We assume that both the unperturbed and perturbed hyperbolic orbital elements are known at some initial time t_i. If the initial time is sufficiently earlier or later than the time of closest approach it might be possible to neglect the perturbations at the

initial time. The perturbed hyperbolic orbital elements at any time t are computed as follows.

1. Propagate the unperturbed orbit from time t_i to time t. This is accomplished by keeping the first five hyperbolic orbital elements the same as at time t_i and applying equation (3) to compute the mean anomaly. Also, infer the values of the hyperbolic true and eccentric anomalies.
2. Apply equations (17) and (26) to compute the functions of the inclinations. Apply equations (19), (21), (23), (27), and (29) to compute the functions of eccentricities. Note that if this calculation is going to be made more than once, both the inclination functions and the factors independent of the mean, true, or eccentric anomalies involved in the equations giving the eccentricities functions can be computed once, using the initial hyperbolic orbital elements.
3. Apply equations (18), (20), (22), (24), (25), and (28) to compute the variations of the hyperbolic orbital elements.
4. Determine the constants of integration from the perturbed orbital elements at the initial time.

5. COMPARISONS WITH OTHER THEORY AND NUMERICAL INTEGRATIONS

We compared the results of section 4 with the results predicted by the AG's theory and with the results of numerical integrations.

The tests presented in this section use a typical Titan flyby of Cassini's trajectory. For Titan, $\mu \approx 8978.173\ \mathrm{km^3 s^{-2}}$, and $R \approx 2575$ km; we took values of C_{20} and C_{22} equal to 4.9×10^{-5} and 1.5×10^{-5}, as estimated in Rappaport *et al.* (1997).

For the flyby considered and at the time of closest approach, the distance from Titan's center is ≈ 4074.9 km and the speed with respect to Titan is ≈ 5.9 km/s; the eccentricity of the hyperbolic orbit is ≈ 14.9, the inclination is $\approx 67.5°$, the longitude of the node is $\approx 202.9°$, the argument of pericenter is $\approx 135.7°$, and the mean anomaly is equal to zero. We assumed that the above coordinates correspond to the unperturbed orbit. For the initial time, we selected two hours before closest approach.

We determined the trajectory analytically with a point every minute implementing the theory presented in this paper as described at the end of section 4.

We also used the AG's theory, as well as a variant of this method, which incorporates an improvement and corrections described below.

We performed numerical integrations by the Burlish and Stoer method, starting at the initial time and taking as initial conditions the perturbed state at that time.

Figures 1 and 2 show the variations in hyperbolic elements as a function of time for four hours centered on closest approach. For any hyperbolic element E among the first five ones, we plotted $\Delta E \equiv E_p(t) - E_p(t_i)$, where the subscript p stands for "perturbed." As far as the mean anomaly is concerned, we defined $\Delta M \equiv M_p(t) - M_p(t_i) - n[a_p(t_i)](t - t_i)$.

In each figure, the solid line corresponds to the numerical integration, the open circles were computed from the new theory of this paper, and the crosses correspond to the AG's theory. For clarity, only one symbol per five points is plotted. The units are kilometers and degrees.

5.1. Effects of the Mass

The first comparison concerns the case where the spacecraft is perturbed only by the satellite mass. The results are shown in Figure 1. These figures show a significant disagreement between the AG and the new theory (or the numerical integration) for all elements except the inclination and longitude of the node.

This disagreement can be eliminated by replacing AG's solution for the perturbations due to the mass by the exact solution. The modified equations for the monopole effect, in function of the six elements p, q, w, b, v, and η used by AG, are

$$
\begin{aligned}
p &= 0, \\
q &= 0, \\
w \equiv w_0 &= \arcsin\left[\frac{\sin f}{\sqrt{1+e^2+2e\cos f}}\right], \\
b &= -\frac{a(e^2-1)}{\sqrt{1+e^2+2e\cos f}}, \\
v &= \frac{v_0}{e+1}\sqrt{1+e^2+2e\cos f}, \\
\eta &= -\frac{ae(e^2-1)\sin f}{(1+e\cos f)\sqrt{1+e^2+2e\cos f}},
\end{aligned}
\tag{31}
$$

where $v_0 \equiv v_p$ is the velocity at closest approach. So, in order to improve the Anderson-Giampieri theory for the mass perturbations, we recommend replacing equations (47) to (51) of their original paper by equations (31) above. Except for this change and an additional change described in section 5.2, the practical implementation of their theory remains the same.

5.2. Effects of C_{20} and C_{22}

We studied the effects of C_{20} and C_{22} separately, but for the purpose of briefness, we present here the combined perturbations due to these two gravity harmonic coefficients. The results of the comparison are shown in Figure 2. For this comparison, we used the improved and corrected (see below) AG's theory. We observe an excellent agreement between the numerical integration and the theory presented in this paper. We observe also a good agreement between the latter (or the numerical integration) and the improved and corrected AG's theory.

Figure 3 shows the magnitude of the perturbations in velocity and in line-of-sight velocity for the same flyby. Again, we find a remarkable agreement between the new

theory and the numerical integration, while the AG's theory is a good approximation of both.

This good agreement was obtained by correcting a number of errors in section 6.2 "Quadrupole Sectorial Harmonics" of the AG's paper. Their equation (66) must be replaced by

$$\dot{r}' = -\frac{3\mu R^2 C_{22}}{r^7}\Big[x(5x^2 - 5y^2 - 2r^2), y(5x^2 - 5y^2 + 2r^2), 5z((x^2 - y^2)\Big]. \tag{32}$$

Consequently, the variations due to the quadrupole sectorial harmonics in their paper must be replaced by:

$$p(t) = -\frac{2\mu R^2 C_{22}}{b_0^3 v_0^2 r_0^3}\Big\{(W_x Q_x - W_y Q_y)(r_0^3 - b_0^3) + (W_x P_x - W_y P_y)(2r_0^2 + b_0^2)\eta_0\Big\}, \tag{33}$$

$$q(t) = -\frac{2\mu R^2 C_{22}}{b_0^3 v_0^2 r_0^3}\Big\{(W_x P_x - W_y P_y)(r_0^3 - b_0^3) + (W_x Q_x - W_y Q_y)(r_0^2 - b_0^2)\eta_0\Big\}, \tag{34}$$

$$\begin{aligned} w(t) = -\frac{\mu R^2 C_{22}}{b_0^3 v_0^2 r_0^5}\Big\{ & 2(P_x Q_x - P_y Q_y)(2r_0^5 - 3b_0^5 + r_0^2 b_0^3) + \\ & \Big[(2P_x^2 + Q_x^2 - 2P_y^2 - Q_y^2)(2r_0^4 + b_0^2 r_0^2) + (3P_x^2 - 3Q_x^2 - 3P_y^2 + 3Q_y^2)b_0^4\Big]\eta_0\Big\}, \end{aligned} \tag{35}$$

$$\begin{aligned} b(t) = \frac{\mu R^2 C_{22}}{b_0^2 v_0^2 r_0^5}\Big\{ & (P_x^2 + 2Q_x^2 - P_y^2 - 2Q_y^2)r_0^5 - (3P_x^2 - 3Q_x^2 - 3P_y^2 + 3Q_y^2)b_0^5 + \\ & (2P_x^2 - 5Q_x^2 - 2P_y^2 + 5Q_y^2)r_0^2 b_0^3 + 2(P_x Q_x - P_y Q_y)(r_0^4 - 3b_0^4 + 2r_0^2 b_0^2)\eta_0\Big\}, \end{aligned} \tag{36}$$

$$\begin{aligned} v(t) = -\frac{\mu R^2 C_{22}}{b_0^3 v_0 r_0^5}\Big\{ & 3(P_x^2 - P_y^2)r_0^5 - (3P_x^2 - 3Q_x^2 - 3P_y^2 + 3Q_y^2)b_0^5 - \\ & 3(Q_x^2 - Q_y^2)r_0^2 b_0^3 - 6(P_x Q_x - P_y Q_y)b_0^4 \eta_0\Big\}, \end{aligned} \tag{37}$$

$$\eta_i(t) = -\frac{\mu R^2 C_{22}}{b_0^2 v_0^2 r_0^5}\Bigg\{2(P_x Q_x - P_y Q_y)(r_0^5 - 6b_0^5 + 5r_0^2 b_0^3) + \Big[(2P_x^2 + Q_x^2 - 2P_y^2 - Q_y^2)r_0^4 + 2(3P_x^2 - 3Q_x^2 - 3P_y^2 + 3Q_y^2)b_0^4 + (P_x^2 + 5Q_x^2 - P_y^2 - 5Q_y^2)r_0^2 b_0^2\Big]\eta_0\Bigg\}. \quad (38)$$

6. EFFECT OF THE ROTATION ON THE PERTURBATIONS DUE TO THE QUADRUPOLE MOMENTS

In this section we come back to the assumption made in section 4.2 that the rotation of the body during the duration of the flyby could be neglected in computing the perturbations due to the body's quadrupole moments. First, we discuss the applicability of this assumption, and then we derive a third modification of the AG's theory, which gets rid of this assumption.

6.1. Applicability of the Assumption that the Body's Rotation can be Neglected

As a rule of thumb, the orbital perturbations are applied over an interval of time $\sim 5b/v$, which is at most of order one hour for Cassini targeted flybys. The duration of gravity experiments is between 2 and 4 times this duration. By comparison, the rotation periods of most Saturnian satellites are equal to their orbital period, which is of order one day or greater for the nine major satellites. Exceptions are Phoebe, which has a period of 9.282 hours (Davies et al. 1996), and Hyperion, whose rotation is chaotic (Wisdom et al. 1984).

Hence, in practice, the assumption made in our work is the least justified for the targeted flyby of Phoebe and for the targeted flybys of Enceladus (there is no targeted flyby of Mimas by Cassini and we are not planning to measure the gravity harmonic coefficients of Hyperion). We compared the variations of the hyperbolic elements for several flybys, in the two cases where we neglect and do not neglect the satellite's

rotation. These tests were based on numerical integrations. The results agree very well, except for the mean anomaly. This is illustrated in the case of the Phoebe flyby (worst case for Cassini) by Figure 4.

In section 5 of this article, we used a typical Titan flyby as an example. In this example, the assumption of neglecting the rotation rate of Titan over four hours, whereas Titan's rotation period is nearly 16 days, was very well justified.

6.2. Effects of a Rotating Body

The perturbations due to C_{20} are not affected by the body's rotation. On the other hand, an S_{22} term must be considered in addition to the C_{22} term, when taking the effect of the rotation into account. In the rotating frame, we have

$$\begin{aligned} C_{22}(t) &= C_{22}^0 \cos(2\omega_r t), \\ S_{22}(t) &= C_{22}^0 \sin(2\omega_r t), \end{aligned} \tag{39}$$

where ω_r is the rotation rate of the body. In the framework of the AG's theory, and assuming that the body rotates around its axis of maximum inertia, the variations due to the time-varying sectorial coefficients are given by:

$$\begin{aligned} p(t) = -\frac{6\mu R^2 C_{22}^0}{b_0^3 v_0^2} \Big\{ & (W_x P_x - W_y P_y)\mathcal{C}(5,0) + (W_x Q_x - W_y Q_y)\mathcal{C}(5,1) + \\ & (W_x P_y + W_y P_x)\mathcal{S}(5,0) + (W_x Q_y + W_y Q_x)\mathcal{S}(5,1) \Big\}, \end{aligned} \tag{40}$$

$$\begin{aligned} q(t) = -\frac{6\mu R^2 C_{22}^0}{b_0^3 v_0^2} \Big\{ & (W_x P_x - W_y P_y)\mathcal{C}(5,1) + (W_x Q_x - W_y Q_y)\mathcal{C}(5,2) + \\ & (W_x P_y + W_y P_x)\mathcal{S}(5,1) + (W_x Q_y + W_y Q_x)\mathcal{S}(5,2) \Big\}, \end{aligned} \tag{41}$$

$$w(t) = -\frac{3\mu R^2 C_{22}^0}{b_0^3 v_0^2}\Big\{ \big(P_x^2 - P_y^2\big)\big(3\mathcal{C}(7,0) - 2\mathcal{C}(7,2)\big) + 5\big(Q_x^2 - Q_y^2\big)\mathcal{C}(7,2) + \\ 2\big(P_xQ_x - P_yQ_y\big)\big(4\mathcal{C}(7,1) - \mathcal{C}(7,3)\big) + \\ 2P_xP_y\big(3\mathcal{S}(7,0) - 2\mathcal{S}(7,2)\big) + 10Q_xQ_y\mathcal{S}(7,2) + \\ 2\big(P_xQ_y + P_yQ_x\big)\big(4\mathcal{S}(7,1) - \mathcal{S}(7,3)\big)\Big\}, \tag{42}$$

$$b(t) = b_0 + \frac{3\mu R^2 C_{22}^0}{b_0^2 v_0^2}\Big\{ \big(P_x^2 - P_y^2\big)\big(3\mathcal{C}(7,1) - 2\mathcal{C}(7,3)\big) + 5\big(Q_x^2 - Q_y^2\big)\mathcal{C}(7,3) + \\ 2\big(P_xQ_x - P_yQ_y\big)\big(4\mathcal{C}(7,2) - \mathcal{C}(7,4)\big) + \\ 2P_xP_y\big(3\mathcal{S}(7,1) - 2\mathcal{S}(7,3)\big) + 10Q_xQ_y\mathcal{S}(7,3) + \\ 2\big(P_xQ_y + P_yQ_x\big)\big(4\mathcal{S}(7,2) - \mathcal{S}(7,4)\big)\Big\}, \tag{43}$$

$$v(t) = v_0 + \frac{3\mu R^2 C_{22}^0}{b_0^3 v_0}\Big\{ 2\big(P_xQ_x - P_yQ_y\big)\big(\mathcal{C}(7,0) - 4\mathcal{C}(7,2)\big) + \\ \big(Q_x^2 - Q_y^2\big)\big(2\mathcal{C}(7,1) - 3\mathcal{C}(7,3)\big) - 5\big(P_x^2 - P_y^2\big)\mathcal{C}(7,1) + \\ 2\big(P_xQ_y + P_yQ_x\big)\big(\mathcal{S}(7,0) - 4\mathcal{S}(7,2)\big) + \\ 2Q_xQ_y\big(2\mathcal{S}(7,1) - 3\mathcal{S}(7,3)\big) - 10P_xP_y\mathcal{S}(7,1)\Big\}, \tag{44}$$

$$\eta_i(t) = -\frac{3\mu R^2 C_{22}^0}{b_0^2 v_0^2}\Big\{ \big(P_x^2 - P_y^2\big)\big(3\mathcal{C}(7,0) - 7\mathcal{C}(7,2)\big) + \\ \big(Q_x^2 - Q_y^2\big)\big(7\mathcal{C}(7,2) - 3\mathcal{C}(7,4)\big) + \\ 10\big(P_xQ_x - P_yQ_y\big)\big(\mathcal{C}(7,1) - \mathcal{C}(7,3)\big) + \\ 2P_xP_y\big(3\mathcal{S}(7,0) - 7\mathcal{S}(7,2)\big) + 2Q_xQ_y\big(7\mathcal{S}(7,2) - 3\mathcal{S}(7,4)\big) + \\ 10\big(P_xQ_y + P_yQ_x\big)\big(\mathcal{S}(7,1) - \mathcal{S}(7,3)\big)\Big\}, \tag{45}$$

with

$$\mathcal{C}(n,m) = X^{m+1} \sum_{p=0}^{+\infty} \frac{(-1)^p (2wt)^{2p}}{(2p)!(m+2p+1)} F\left[\frac{n}{2}, \frac{m+2p+1}{2}, \frac{m+2p+3}{2}; -X^2\right], \quad (46)$$

$$\mathcal{S}(n,m) = X^{m+1} \sum_{p=0}^{+\infty} \frac{(-1)^p (2wt)^{2p+1}}{(2p+1)!(m+2p+2)} F\left[\frac{n}{2}, \frac{m+2p+2}{2}, \frac{m+2p+4}{2}; -X^2\right], \quad (47)$$

where

$$X = \frac{vt}{b}, \quad (48)$$

and F[a,b,c;x] is a hypergeometric function (Abramowitz and Stegun 1970). Note that equations (33) to (38) can be obtained from equations (40) to (45) as the zero-th order terms in the expansion of powers of $\omega_r t$.

7. CONCLUSION

In this paper, we have developed an analytical theory for the perturbations of a spacecraft due to the gravity coefficients C_{20} and C_{22}. Comparisons with numerical integrations show that this theory is very accurate.

The hyperbolic theory described here can be applied in general for flybys of both icy satellites and giant planets, unlike a previous theory based on the Born approximation, which required that μ/bv^2 be small (see AG 1999). We compared the new theory with the one developed by Anderson and Giampieri. We found that we could get a good agreement between the two theories for icy satellites provided that we modify the AG's theory to compute accurately the perturbations due to the mass and that a sign error in the C_{22} part of the potential function (Eq. 66 of the AG's theory) be corrected to read (32).

APPENDIX A

A.1. Reference Frames

A.1.1. Body-Fixed Reference Frame at Closest Approach

We consider the hyperbolic orbit of a spacecraft flying by a punctual satellite at O. We denote by $Oxyz$ the satellite body-fixed reference frame at closest approach.

A.1.2. Orbital Frames

At any time, the orbital frame is such that the Ox'-axis is in the direction of periapsis and the Oz'-axis is normal to the orbit. This frame can be obtained from the body-fixed frame at closest approach by three Euler rotations with angle:

1) Ω = longitude of the ascending node;

2) I = inclination of the orbit;

3) ω = argument of pericenter.

The matrix of passage from $Oxyz$ to $Ox'y'z'$ is

$$M(\Omega, I, \omega) = \begin{pmatrix} \cos\Omega\cos\omega - \cos I\sin\Omega\sin\omega & \sin\Omega\cos\omega + \cos I\cos\Omega\sin\omega & \sin I\sin\omega \\ -\cos\Omega\sin\omega - \cos I\sin\Omega\cos\omega & -\sin\Omega\sin\omega + \cos I\cos\Omega\cos\omega & \sin I\cos\omega \\ \sin I\sin\Omega & -\sin I\cos\Omega & \cos I \end{pmatrix}. \quad (49)$$

A.1.3. Orbital Frame at Closest Approach

The orbital frame at closest approach ($t = t_{c/a}$) is a particular case of orbital frame. Let us call $M_{c/a}$ the matrix of passage from $Oxyz$ to $Ox'_{c/a}y'_{c/a}z'_{c/a}$.

We define the variables p, q, and w_1 which orient the orbital frame $Ox'y'z'$ at time t with respect to the orbital frame $Ox'_{c/a}y'_{c/a}z'_{c/a}$ at closest approach through tree rotations around the $x'_{c/a}$-, $y'_{c/a}$- and $z'_{c/a}$−axes. The matrix of passage from $Ox'_{c/a}y'_{c/a}z'_{c/a}$ to $Ox'y'z'$ is:

$$\hat{M} = \begin{pmatrix} \cos q \cos w_1 & -\cos q \sin w_1 & \sin q \\ \sin p \sin q \cos w_1 + \cos p \sin w_1 & -\sin p \sin q \sin w_1 + \cos p \cos w_1 & -\sin p \cos q \\ \cos p \sin q \cos w_1 + \sin p \sin w_1 & \cos p \sin q \sin w_1 + \sin p \cos w_1 & \cos p \cos q \end{pmatrix}. \tag{50}$$

We must have

$$\hat{M} = M^T_{c/a} \times M. \tag{51}$$

To first order in p, q and w_1, we have

$$\hat{M} = \begin{pmatrix} 1 & -w_1 & q \\ w_1 & 1 & -p \\ q & p & 1 \end{pmatrix}. \tag{52}$$

A.2. Hyperbolic Elements

A.2.1. Classical Hyperbolic Elements

From Eqs. 4-61, page 170, of Battin (1987), the position and velocity in the orbital frame are given by

$$\begin{aligned} \vec{r} &= a(\cosh H - e)\hat{e_{x'}} + \sqrt{-ap}\sinh H \hat{e_{y'}}, \\ \vec{v} &= -\frac{\sqrt{-\mu a}}{r}\sinh H \hat{e_{x'}} + \frac{\sqrt{\mu p}}{r}\cosh H \hat{e_{y'}}, \end{aligned} \tag{53}$$

$p = -a(e^2 - 1)$; $\hat{e_{x'}}$ and $\hat{e_{y'}}$ are the unit vectors along the Ox'- and Oy'-axes, respectively.

We call H the hyperbolic eccentric anomaly. It is related to the true anomaly f by:

$$\tan\frac{1}{2}f = \sqrt{\frac{e+1}{e-1}}\tanh\frac{1}{2}H. \tag{54}$$

We also have

$$\begin{aligned}
\sin f &= \frac{\sinh H\sqrt{e^2-1}}{(e\cosh H - 1)}, \\
\cos f &= \frac{e - \cosh H}{(e\cosh H - 1)}, \\
\sinh H &= \frac{\sin f\sqrt{e^2-1}}{(1+e\cos f)}, \\
\cosh H &= \frac{e+\cos f}{(1+e\cos f)}.
\end{aligned} \tag{55}$$

Eq. 4-58, page 168, of Battin (1987) relates the hyperbolic eccentric and mean anomalies:

$$M = e\sinh H - H. \tag{56}$$

Using Eq. (53), the radius is

$$r = a(1 - e\cosh H), \tag{57}$$

and the velocity is

$$v = \sqrt{\mu\left(\frac{2}{r} - \frac{1}{a}\right)} = \sqrt{v_\infty^2 + \frac{2\mu}{r}}, \tag{58}$$

where

$$v_\infty = \sqrt{\frac{-\mu}{a}} = -na, \tag{59}$$

is the velocity at infinity. Eq. (59) defines the semi-major axis

$$a = -\frac{\mu}{v_\infty^2}. \tag{60}$$

The radius and velocity at closest approach are given by

$$r_p = a(1-e), \tag{61}$$

and

$$v_p = \sqrt{\frac{e+1}{e-1}} v_\infty = -na\sqrt{\frac{e+1}{e-1}}. \tag{62}$$

By combining Eqs. (60) and (61) we find the eccentricity

$$e = 1 + \frac{r_p v_\infty^2}{\mu}. \tag{63}$$

A.2.2. Anderson-Giampieri Elements

The variables appearing in the matrices (50) and (52) are related to the variables of the AG's theory. More specifically, p and q are the same variables as in this theory and

$$w = w_0 + w_1, \tag{64}$$

where w_0 is given by Eq. (31).

The three other elements used by Anderson and Giampieri, b, v and η are such that v is the velocity as in Eq. (58) and b is the impact parameter. We have:

$$\begin{aligned} v &= |\vec{v}|, \\ \eta &= \frac{\vec{r}\cdot\vec{v}}{v}, \qquad , \\ b &= |\vec{r} - \eta\vec{v}/v|. \end{aligned} \tag{65}$$

REFERENCES

Abramowitz, M., and I.A. Stegun 1970: Handbook of Mathematical Functions With Formulas, Graphs, and Mathematical Tables, U.S. Department of Commerce, National Bureau of Standards, Applied Mathematics Series 55.

Anderson, J.D., W.L. Sjogren, and G. Schubert 1996a: "Galileo Gravity Results and the Internal Structure of Io," *Science* **272**, 709–712.

Anderson, J.D., E.L. Lau, W.L. Sjogren, G. Schubert, and W.B. Moore 1996b: "Gravitational Constraints on the Internal Structure of Ganymede," *Nature* **384**, 541–543.

Anderson, J.D., E.L. Lau, W.L. Sjogren, G. Schubert, and W.B. Moore 1997a: "Gravitational Evidence for an Undifferentiated Callisto," *Nature* **387**, 264–266.

Anderson, J.D., E.L. Lau, W.L. Sjogren, G. Schubert, and W.B. Moore 1997b: "Europa's Differentiated Internal Structure: Inferences from Two Galileo Encounters," *Science* **276**, 1236–1239.

Anderson, J.D. and G. Giampieri 1999: "Theoretical Description of Spacecraft Flybys by Variation of Parameters," *Icarus* **138**, 309–318.

Battin, R.H. 1987: An Introduction to the Mathematics and Methods of Astrodynamics, AIAA Education Series, New York, New York.

Davies, M.E., V.K. Abalakin, M. Bursa, J.H. Lieske, B. Morando, D. Morrison, P.K. Seidelmann, A.T. Sinclair, B. Yallop, and Y.S. Tjuflin 1996: "Report of the IAU/IAG/COSPAR Working Group on Cartographic Coordinates and Rotational Elements of the Planets and Satellites: 1994," *Celestial Mechanics and Dynamical Astronomy* **63**, 127–148, 1996.

Gooding, R.H. 1992: "Untruncated Satellite Perturbations in a Nonrotating Gravitational Field," *Journal of Guidance, Control and Dynamics* **15** 1397–1405.

Kaula, W.M. 1966: Theory of Satellite Geodesy, Blaisdell Publishing Company.

Rappaport, N., B. Bertotti, G. Giampieri, and J.D. Anderson 1997: "Doppler Measurements of the Quadrupole Moments of Titan," *Icarus* **126**, 313–323.

Wisdom, J. S.J. Peale, and F. Mignard 1984: "The chaotic rotation of Hyperion," *Icarus* **58**, 137–152.

FIGURE CAPTIONS

FIGURE 1: Behavior of the hyperbolic elements as a function of time due to the effect of the satellite's mass alone, and computed by three methods (numerical integration, the analytical theory presented in this paper, AG's theory). Units are kilometers and degrees.

FIGURE 2: Variations of the hyperbolic elements as a function of time due to the harmonic gravity coefficients C_{20} and C_{22}, and computed by three methods (numerical integration, the analytical theory presented in this paper, AG's theory). Units are kilometers and degrees.

FIGURE 3: Variations in the spacecraft speed and in the line-of-sight speed due to C_{20} and C_{22} and computed by three methods (numerical integration, the analytical theory presented in this paper, AG's theory). Unit is kilometer per second.

FIGURE 4: Variations of the hyperbolic elements for the Cassini Phoebe flyby, computed in neglecting (solid line) and not neglecting (circles) the rotation of that body. Units are kilometers and degrees.

FIGURE 1

Titan flyby of 2006 Dec. 28

μ

Solid line = numerical integration, circles = this paper theory, crosses = Anderson–Giampieri theory

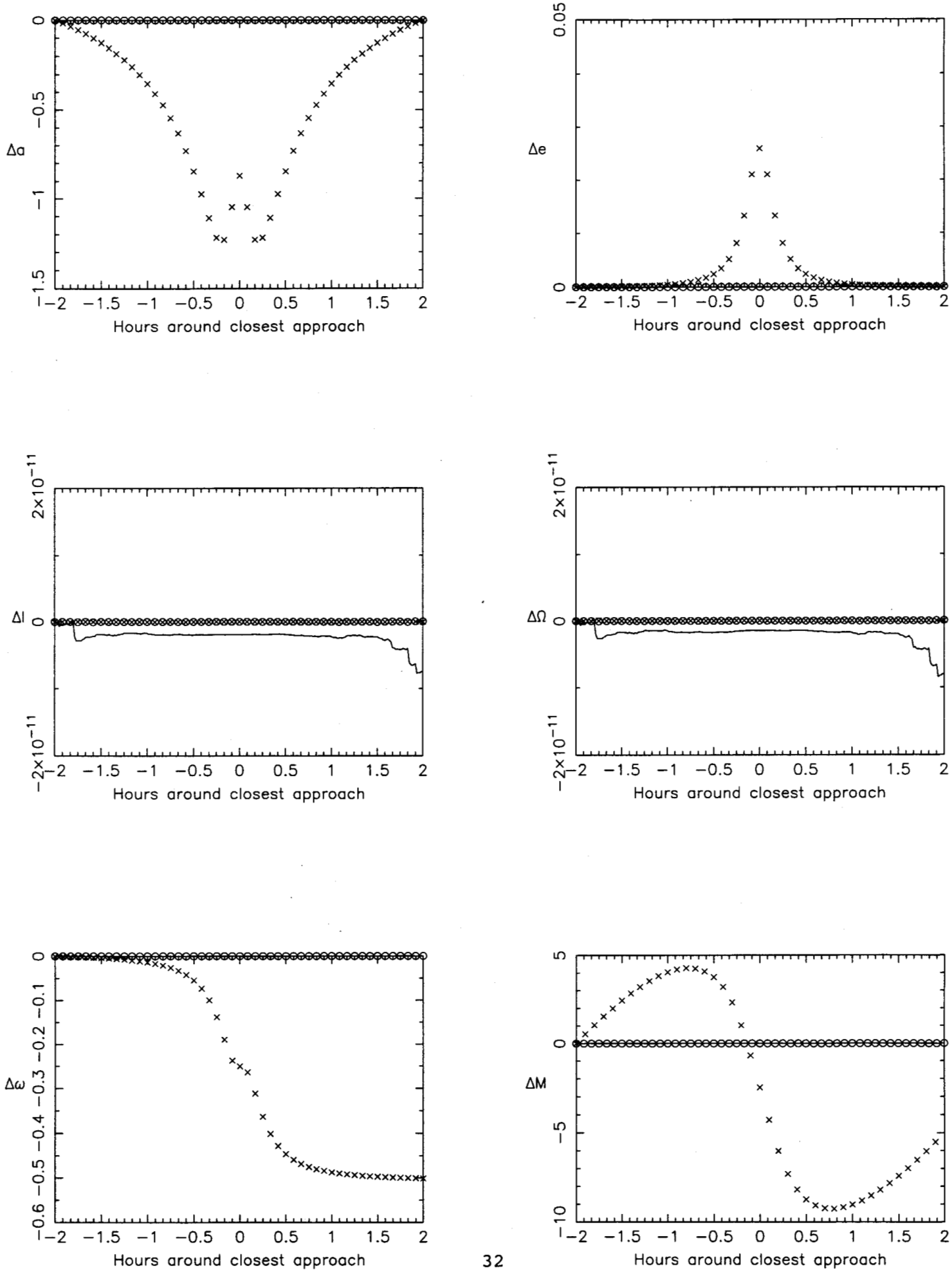

FIGURE 2

Titan flyby of 2006 Dec. 28
C20 + C22
Solid line = numerical integration, circles = this paper theory, crosses = Anderson–Giampieri theory

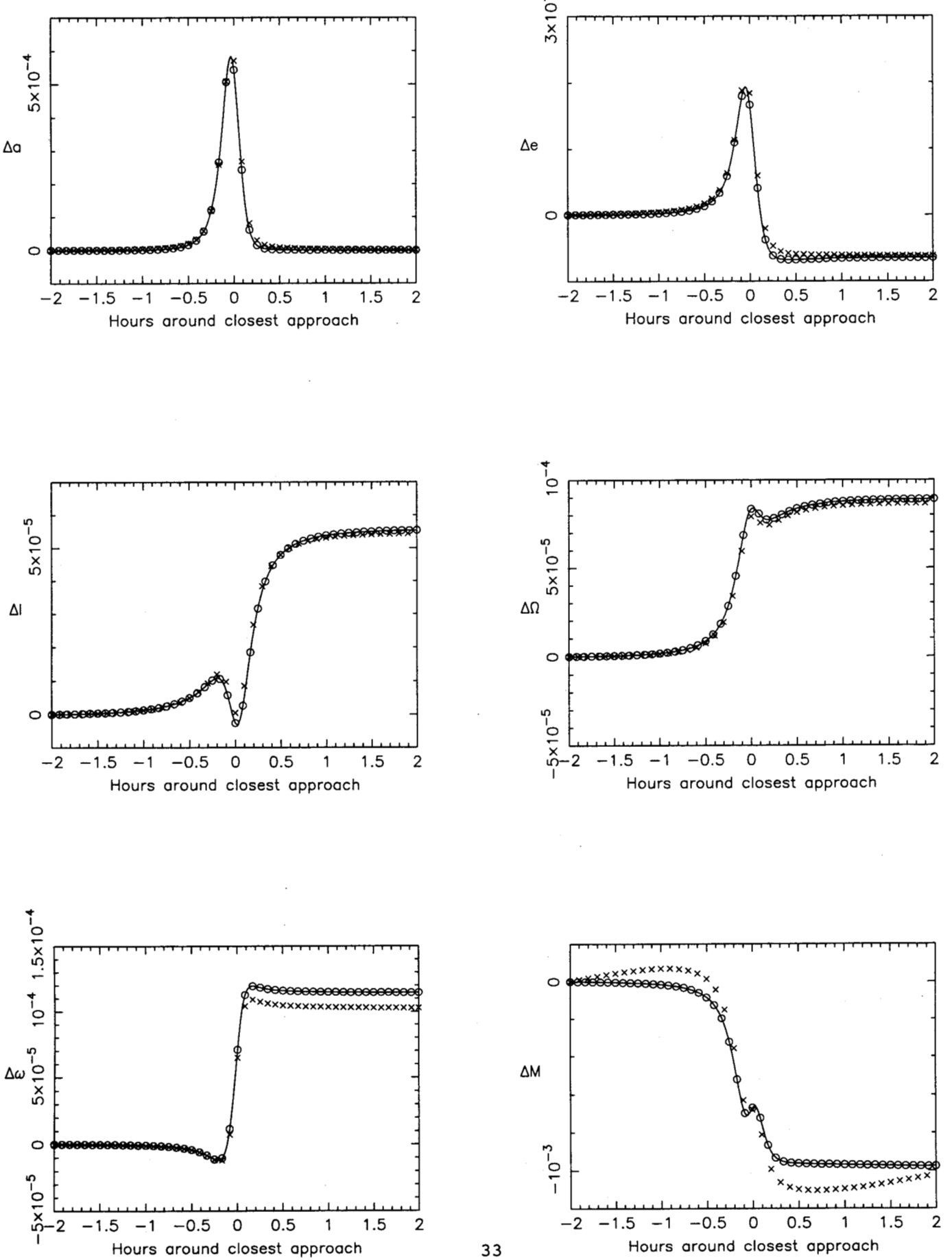

FIGURE 3

Titan flyby of 2006 Dec. 28
C20 + C22
Solid line = numerical integration, circles = this paper theory, crosses = Anderson–Giampieri theory

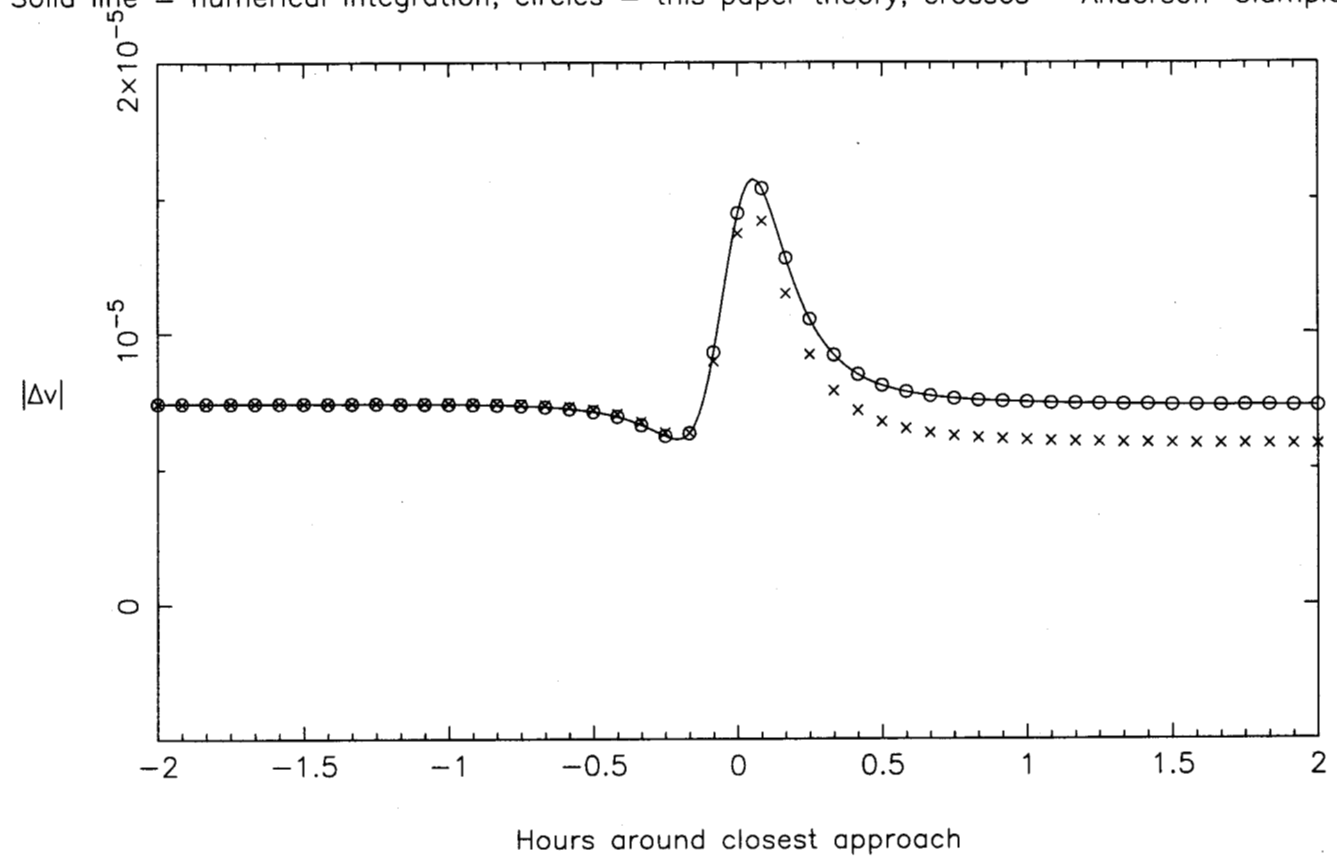

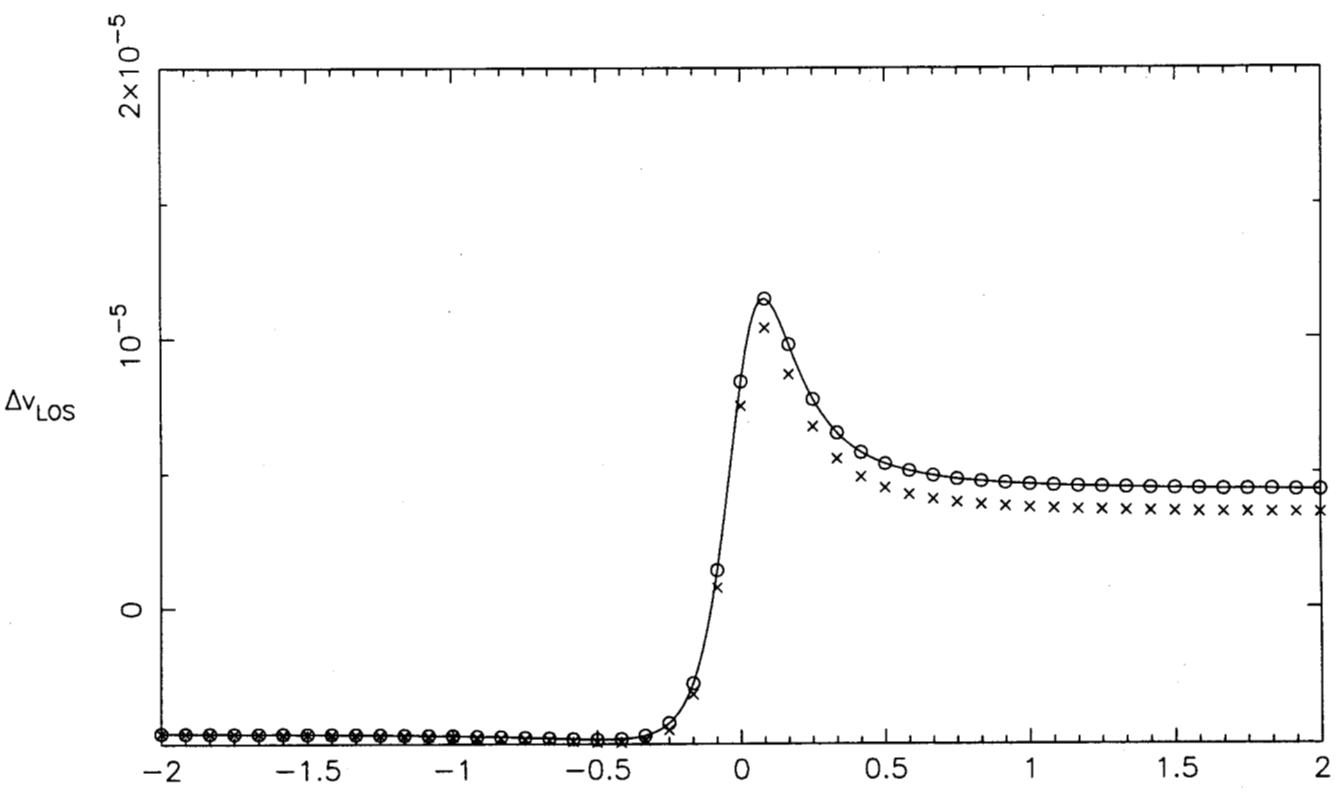

FIGURE 4

Phoebe flyby
C20 + C22
Solid line = neglecting rotation, circles = not neglecting it